26th ABCM International Congress of Mechanical Engineering
November 22-26, 2021. Florianópolis, SC, Brazil

COB-2021-1581
NUMERICAL ANALYSIS OF TENSION AND STABILITY IN COMPRESSION COIL SPRINGS BY THE FINITE ELEMENTS METHOD

Pierre Breno Nunes de Assis
Beatriz da Costa Lima
Laura Fernanda Pereira da Silva
Claudecir Fernandes de Freitas Moura Júnior
Ramon Rudá Brito Medeiros
Universidade Federal do Ceará, Rua Felipe Santiago – N° 411, Cidade Universitária, Russas, CEP 62900-000.
pierrenunes@alu.ufc.br; beatrizdacosta@alu.ufc.br; laura.fernanda@alu.ufc.br; cjunior14@alu.ufc.br; ramon.ruda@ufc.br.

Abstract: *Coil compression springs, when loaded, experience shear and torsional stresses. Due to the curvature of the turns, the stresses in the inner regions are amplified. Analogous to columns, coil compression springs can fail due to buckling. Thus, the objective of this paper is to carry out, through the finite element method, the determination of the factor that correlates the effects of direct shear and stress concentration due to the curvature of the turns and to perform stability analyzes related to buckling in wire springs of circular and square section. For both sections, the stress analysis performed showed a high-stress amplification factor for low spring rates. For higher spring indexes, the factor showed a reduction. The buckling analysis for circular and square sections, with a free end for rotation perpendicular to the longitudinal axis, showed greater susceptibility to unstable behavior for higher free length and turn diameter ratios. Both sections, with both ends crimped, exhibited values susceptible to buckling failure for the ratio between 7 and 10. The results were compared with other studies to understand how the numerical analyses behave in relation to literature data.*

Keywords: *Helical Compression Spring, Stress Concentration, Buckling, Finite Element Method*

1. INTRODUCTION

Coil compression springs are commonly used in industrial and automotive mechanical systems, with the main function of storing and releasing potential energy within the system (Rao, 2016). Its applications range from compressors, pneumatic valves to electrical switches. Generally, steel is the most used raw material for its manufacture, and its shape is usually cylindrical, which may vary if there is a need for a greater load capacity, including square, rectangular and other wires. According to Norton (2013), the ideal material for manufacturing springs must have good mechanical properties, such as high tensile strength, high yield point, and low modulus of elasticity, providing maximum energy storage.

Coil compression springs are designed to accumulate potential elastic energy during their compression movement, in which the absorbed energy is dissipated or used for moving mechanisms. During this movement, due to the applied loads, the coils undergo transverse shear and torsional stress. It is noteworthy that the tensions in the internal region are amplified due to the curvature of the turns. Wahl (1944) reported this phenomenon and defined a multiplicative factor that takes this phenomenon into account through a materials resistance approach.

Henrici (1955) proposed a series solution for the differential equation governing the distribution of stresses in a statically charged helical spring through the modification of a series of Legendre functions appropriated by Freiberger. This study showed that the exact values of the stress concentration factor could be developed in terms of a specific parameter, the spring index.

Cornwell (2006) studied stress concentration factors for springs with different profiles, such as circular and rectangular cross-sections and I-beam profiles, using the finite element method, analyzing the feasibility of applying the Wahl stress concentration factor for low spring rates. Their studies have shown that the Wahl factor can be applicable for indices as low as 1.2, thus providing stress concentration factors for a wider range of cross-section geometries and lower spring indices.

This study aims to perform, through the finite element method (F.E.M.), the determination of the factor that correlates the effects of direct shear and the stress concentration due to the curvature of the spring turns. In addition, perform stability analysis related to buckling in springs with wire with circular and square sections.

2. BIBLIOGRAPHIC REVIEW

2.1 Compression helical springs

Norton (2013) claims that the term 'spring' refers to parts particular built-in configurations to provide a range of force within a significant deflection space and/or to store potential energy. Therefore, they are responsible, mainly for storing potential energy and then releasing it for the execution of a certain movement. Regarding the physical configuration of the springs, considering the wire springs, they can be classified as helical compression springs, helical traction springs, helical torsion springs, and special shapes.

Compression helical springs are the most commonly used, having high deflection capacity. They are found in almost all mechanical products, such as valve return springs in engines, matrix springs, and compressors.

Among the main types of compression helical springs, there is cylindrical, conical (barrel-shaped), hourglass-shaped, variable, or constant pitch. Moreover, the coils that constitute it can be either right or left hand. To define the geometry of the springs for calculation and manufacturing purposes, the main variables (Fig. 1) used are wire diameter (d), average coil diameter (D), free length in the unloaded force condition (L_f), and the number of coils (N_t) or the step of coils (p) (Norton, 2013).

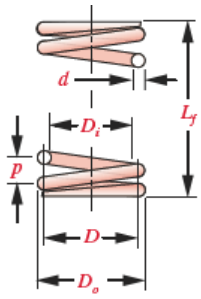

Figure 1. Geometric parameters of the compression helical spring (Norton, 2013).

An important factor in defining the characteristics of spring is known as the spring index (C), defined by Eq. (1).

$$C = \frac{D}{d} \tag{1}$$

It is preferable that C is contained in the range $4 \leq C \leq 12$ because values lower than 4 indicate difficult-to-manufacture springs, and higher than 12, springs prone to buckling.

2.1.1 Stresses in compression helical springs

In each cross-section of a coil, there will be two stress components: one of torsional shear (Fig. 2a), due to a torque T; and one of transverse shear (Fig. 2b), due to a shear force F (resulting from internal forces associated with an external force F applied in the axial direction).

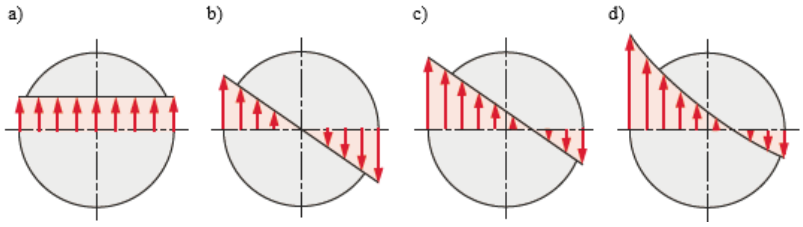

Figure 2. Stress distribution along the cross-section of a wire. (a) Transverse shear distribution (b) Torsional shear distribution (c) Combined stresses (d) Effect of stress concentration (adapted from Norton, 2013).

Figure 2c shows the resulting stress state, disregarding the curvature of the coils. However, the maximum stress is increased (Fig. 2d) due to this curvature. Through a materials strength approach, Wahl (1944) developed the expression Eq. (2) to calculate the maximum shear stress considering the curvature of the coil.

$$\tau_{max} = \frac{8.F.D}{\pi.d^3}.\left(\frac{4.C-1}{4.C-4}+\frac{0{,}615}{C}\right) = K.\frac{8.F.D}{\pi.d^3} \quad (2)$$

Henrici (1955), through the series solution of the differential equation that governs the problem, obtained the expression Eq. (3) for the maximum shear stress in springs with circular wire section.

$$\tau_{max} = \frac{8.F.D}{\pi.d^3}.\left(1+\frac{5}{4.C}+\frac{7}{8.C^2}+\frac{155}{256.C^3}+\frac{11911}{24576.C^4}\right) = K.\frac{8.F.D}{\pi.d^3} \quad (3)$$

Cornwell (2006), through a finite element analysis, obtained the expression Eq. (4) for the maximum shear stress in springs with circular wire section and the expression Eq. (5) for the maximum shear stress in springs with square wire section.

$$\tau_{max} = \frac{8.F.D}{\pi.d^3}.\left\{e^{[2{,}2052-3{,}9819.lnC+3{,}5237.(lnC)^2-1{,}5013.(lnC)^3+0{,}2697.(lnC)^4]}\right\} = K.\frac{8.F.D}{\pi.d^3} \quad (4)$$

$$\tau_{max} = \frac{8.F.D}{\pi.d^3}.\left\{e^{[1{,}6844-2{,}8219.lnC+2{,}4577.(lnC)^2-1{,}0591.(lnC)^3+0{,}1721.(lnC)^4]}\right\} = K.\frac{8.F.D}{\pi.d^3} \quad (5)$$

2.1.2 Stability in compression helical springs

Simply put, it can be said that a helical compression spring is loaded force as a column and, depending on the ratio between length and the diameter of the coil, it may undergo buckling. Therefore, the slenderness factor parameter that considers the ratio between the free length and the diameter of the coil, L_f/D, was developed to analyze the buckling in compression helical springs. This factor was called the aspect ratio (Norton, 2013).

If this factor is greater than 4, the spring may buckle. Among the aspects that influence this situation, the end conditions of the springs can affect their tendency to buckling. A spring with parallel ends, with one set fixed and the other restricted by parallelism, has a lower probability of buckling than a spring in the condition of non-parallel ends, with one end set fixed and the other free to rotate (Norton, 2013).

Another factor affecting the trend of spring to buckling is the ratio between the deflection of the spring and its free length and may be termed the deflection ratio. Figure 3a shows the results obtained by *Associated Spring Design - A.S.D.* (1987), and Figure 3b presents the results obtained by Haringx (1948).

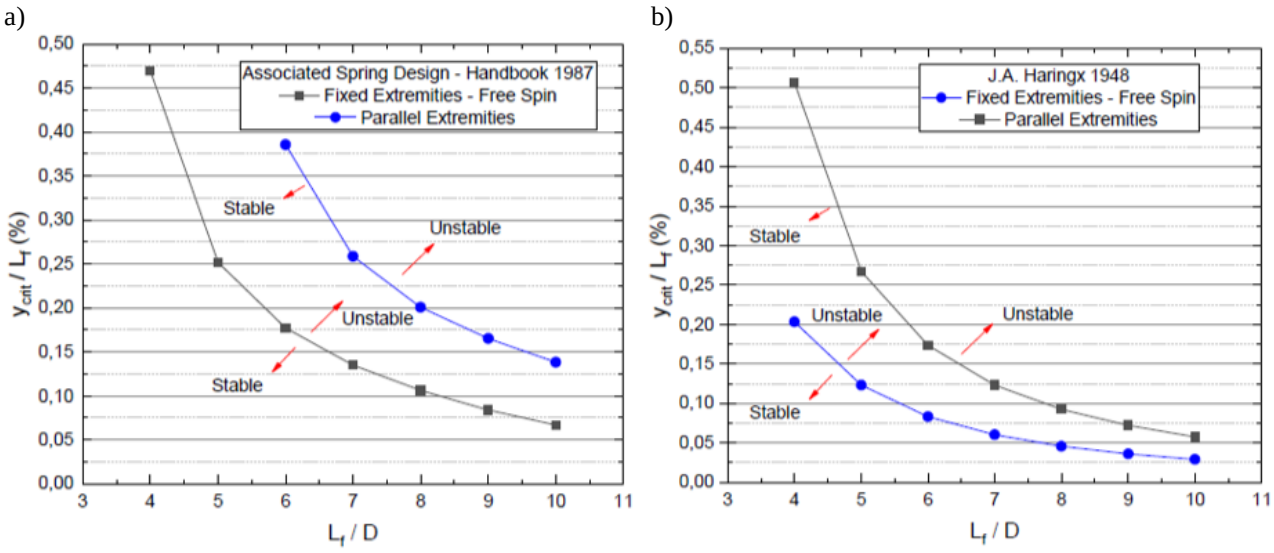

Figure 3. a) Buckling critical stability curve (*Associated Spring Design Handbook*, 1987). b) Buckling critical stability curve (J.A. Haringx, 1948).

2.1.3 Finite element method

According to Logan (1992), the finite element method (F.E.M.) is a numerical method to solve engineering problems. Formulating a problem by this method results in a system of simultaneous algebraic equations for the solution. Simply put, the process of modeling a body is done by dividing it into an equivalent system of smaller bodies or units (finite elements) interconnected at points common to two or more elements (nodal points or nodes) and/or surface lines forming the meshes. This modeling is called discretization (Alves Filho, 2012).

In order to simplify the formulation of the rigidity equations of the elements, matrix methods are a necessary tool used in F.E.M., as this notation represents a simple and easy way to write and solve sets of algebraic equations. The linear analysis is based on the expression of Eq. (6).

$$\{F\} = [K]\{U\} \tag{6}$$

In this notation, $\{F\}$ is a column matrix with all nodal loads forces, $[K]$ is a square rigidity matrix relating all nodal displacements to nodal loads forces, and $\{U\}$ is a column matrix with all nodal displacements. (Haubert, 2017)

The formulation of buckling linear analysis is expressed by equation Eq. (7).

$$([K] + \lambda_i[S]).\{\psi\}_i = \{0\} \tag{7}$$

This formulation deals with an eigenvalue problem where the objective is to obtain the smaller positive eigenvalue. The terms that appear in Eq. (7) are: $[K]$ rigidity matrix, $[S]$ stress rigidity matrix, λ_i the eigenvalues, and $\{\psi\}_i$ the displacement eigenvectors (Ansys, 2021). Once the equation is solved using algorithms, the smaller eigenvalue λ of positive value is used to determine the buckling critical load force employing Eq. (8). It is noteworthy that the load force F is the load force used to generate the strain state represented by the matrix $[S]$.

$$P_{crit} = \lambda_i.F \tag{8}$$

3. METHODOLOGY

The work will be divided into four different analyses. First, tension analyzes will be performed on springs with circular and square sections wires, using the same boundary conditions. Later, adopting the same types of cross-sections, the buckling analysis will be performed. Numerical analyzes will be performed in the student version of ANSYS ACADEMIC 2021® software.

Stress analyses will be restricted to springs with a spring index (C) in the range $2.5 \leq C \leq 10$, and buckling analysis will be restricted to springs with $3 \leq L_f/D \leq 10$.

3.1 Stress analysis

From the geometry parameterization, seven design points with distinct geometry will be obtained. After modeling and simulation, the maximum shear stress will be returned. Each spring will be constructed so that it has both simple ends (Norton, 2013). The same boundary conditions, Figure 4, will be applied to both the circular and square sections. At one end of the spring, there will be a condition of fixed support in the center of the coil, and at the other end, a compressive load of 100 N (applied to the center of the coil).

a) b)

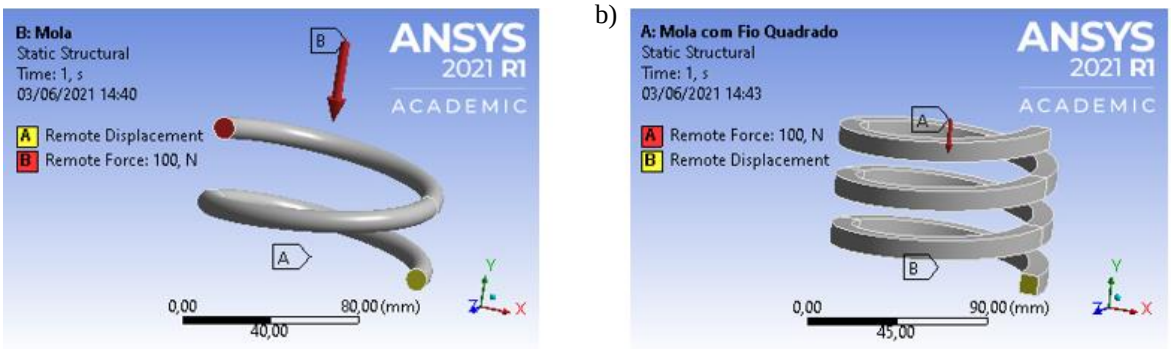

Figure 4. Boundary conditions applied in stress analysis. a) Wire spring with a circular cross-section. b) Wire spring with a square cross-section (Own Authorship, 2021).

3.1.1 Spring with circular section wire

As already mentioned, seven geometries with distinct spring rates were selected from the range described above. Table 1 illustrates the geometric parameters adopted for springs with circular section wire.

Table 1. Geometric parameters for stress analysis for spring with circular section wire.

Geometry	d (m)	D (m)	C (D/d)	$L_f - d$ (m)	N_a
1	0.0100	0.0250	2.5000	0.05	1.50
2	0.0100	0.0375	3.7500	0.05	1.50
3	0.0100	0.0500	5.0000	0.05	1.50
4	0.0100	0.0625	6.2500	0.05	1.50
5	0.0100	0.0750	7.5000	0.05	1.50
6	0.0100	0.0875	8.7500	0.05	1.50
7	0.0100	0.1000	10.0000	0.05	1.50

The mesh for this modeling will be composed of hexahedral quadratic elements with a size of 0.0017 m. This size was selected to respect the ANSYS ACADEMIC 2021 ® limitation (128,000 nodes or elements) and will be maintained for all design points.

3.1.2 Wire spring with square section

As already mentioned, seven geometries with distinct spring rates were selected from the range described above. Table 2 illustrates the geometric parameters adopted for springs with square section wire.

Table 2. Geometric parameters for stress analysis for square-section wire spring.

Geometry	l (m)	D (m)	C (D/l)	$L_f - l$ (m)	N_a
1	0.0100	0.0250	2.5000	0.075	3.00
2	0.0100	0.0375	3.7500	0.075	3.00
3	0.0100	0.0500	5.0000	0.075	3.00
4	0.0100	0.0625	6.2500	0.075	3.00
5	0.0100	0.0750	7.5000	0.075	3.00
6	0.0100	0.0875	8.7500	0.075	3.00
7	0.0100	0.1000	10.0000	0.075	3.00

The mesh for this modeling will be composed of hexahedral quadratic elements with a size of 0.0017 mm. This size was selected to respect the ANSYS ACADEMIC 2021 ® limitation (128,000 nodes or elements) and will be maintained for all design points.

3.2 Buckling Analysis

From the parameterization of the geometry, eight design points with distinct geometry will be obtained. After modeling and simulation, the deflection (y) and load multiplier factor (λ_i) will be returned. The critical buckling load is given by Eq. (8). Considering that the spring has a linear elastic behavior, the critical buckling deflection will be calculated by Eq. (9).

$$y_{crit} = \lambda_i . y \tag{9}$$

Each spring will be constructed so that it has both simple ends (Norton, 2013). The same boundary conditions, figure 5, will be applied to both cross-sections. Two distinct boundary conditions will be applied to determine the critical load and deflection of buckling. In the first condition, at one end of the spring, there will be a condition of fixed support in the center of the coil, and at the other end, a compressive load of 200 N will be applied to the center of the coil. In addition, the only displacement along the longitudinal axis and rotation on an axis perpendicular to the longitudinal axis will be allowed at the load application end.

In the second condition, there will be the condition of fixed support in the center of the coil, while at the other, a compressive load of 200 N will be applied to the center of the coil. Furthermore, at the load application end, displacement along the longitudinal axis will be allowed.

a) b)

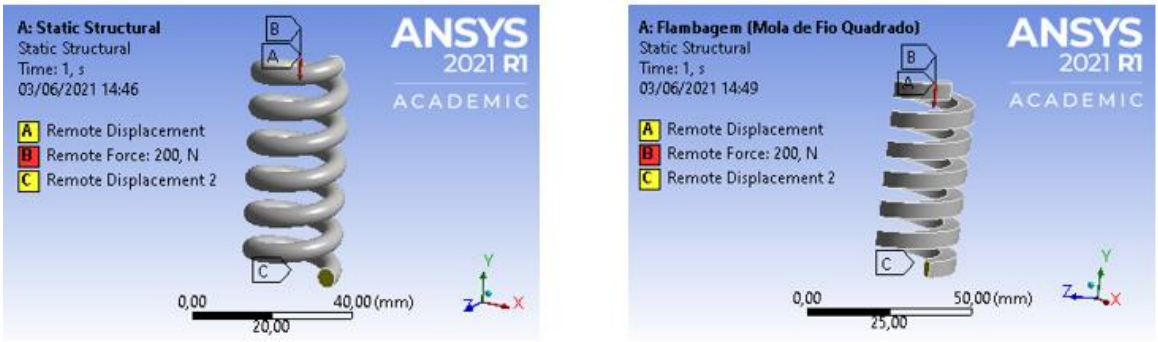

Figure 5. Boundary conditions were applied in the buckling analysis. a) Wire spring with a circular cross-section. b) Wire spring with a square cross-section (Own Authorship, 2021).

3.2.1 Spring with circular wire section

Analogous to stress analysis, eight geometries with distinct L_f/D ratios were selected in the range described above. Table 3 illustrates the geometric parameters adopted for springs with circular section wire.

Table 3. Geometric parameters for buckling analysis for spring with circular section wire.

Geometry	d (m)	D (m)	N_a	L_f (m)	L_f / D
1	0.005	0.020	6.00	0.060	3.00
2	0.005	0.020	8.00	0.080	4.00
3	0.005	0.020	10.00	0.100	5.00
4	0.005	0.020	12.00	0.120	6.00
5	0.005	0.020	14.00	0.140	7.00
6	0.005	0.020	16.00	0.160	8.00
7	0.005	0.020	18.00	0.180	9.00
8	0.005	0.020	20.00	0.200	10.00

The mesh for this modeling will be composed of hexahedral quadratic elements with a size of 0.0025 mm. This size was selected to have a comparative basis with the results obtained for the circular section and will be maintained for all design points.

3.2.2 Spring with square wire section

Analogous to stress analysis, eight geometries with distinct L_f/D ratios were selected in the range described above. Table 4 illustrates the geometric parameters adopted for springs with square section wire.

Table 4. Geometric parameters for buckling analysis for spring with square section wire.

Geometry	d (m)	D (m)	N_a	L_f (m)	L_f/D
1	0.005	0.020	6.00	0.060	3.00
2	0.005	0.020	8.00	0.080	4.00
3	0.005	0.020	10.00	0.100	5.00
4	0.005	0.020	12.00	0.120	6.00
5	0.005	0.020	14.00	0.140	7.00
6	0.005	0.020	16.00	0.160	8.00
7	0.005	0.020	18.00	0.180	9.00
8	0.005	0.020	20.00	0.200	10.00

The mesh for this modeling will be composed of hexahedral quadratic elements with a size of 0.0025 mm. This size was selected in order to have a comparative basis with the results obtained for the square section and will be maintained for all design 'points.

4. RESULTS AND DISCUSSIONS

4.1 Stress analysis

The stress amplification factor due to direct shear and stress concentration for circular section wire (Fig. 6a), in general, presented high values for low spring indexes, while for higher spring indexes, the factor presented decline. The numerical analysis (F.E.M.) showed higher stress amplification factors compared to the studies by Wahl (1944), Henrici (1955), and Cornwell (2006), regardless of the spring curvature index studied. It can be observed that the higher the spring index, the greater the discrepancy between the numerical study and the other analytical models. It is noteworthy that these results followed a study of mesh convergence, however, based on the limitations of the student version of the software.

The analytical study by the method of Henrici (1955) and Cornwell (2006) showed good convergence for spring indices with values of 2.5, 6.25, and 10, indicating an average difference of 3.72%, 1.82%, and 1.62% compared to Henrici and 3.34%, 1.56%, and 1.34% compared to Cornwell. The analysis by the method of Wahl (1944), for the spring curvature indices 2.5, 6.25, 7.50, 8.75, and 10 showed higher values about the methods mentioned above, thus becoming, among the analyzes considered from the literature, the more conservative. Equation 10 adjusts the data obtained in the present study to the stress amplification factor for the spring with circular section wire.

$$K = e^{[1{,}3760-1{,}2990.lnC+0{,}5546.(lnC)^2-0{,}1288.(lnC)^3+0{,}0139.(lnC)^4]} \quad (10)$$

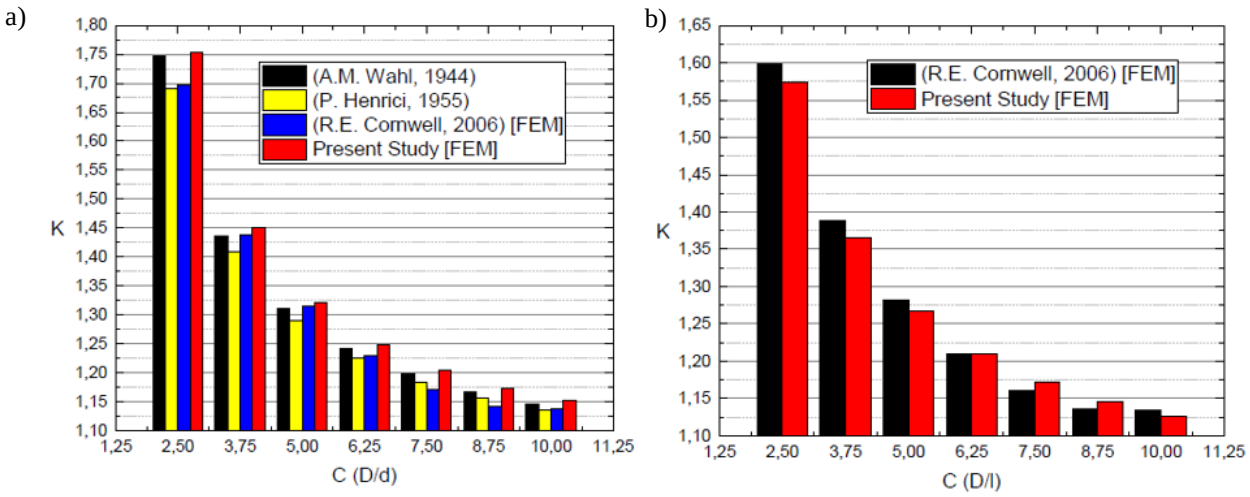

Figure 6. Stress amplification factor due to direct shear and curvature index. a) Wire spring with a circular cross-section. b) Square cross-section wire spring (Own Authorship, 2021).

The stress amplification factor due to direct shear and stress concentration for square section wire (Fig. 6b), in general, also presented high values for low spring indexes, while for higher spring indexes, the factor showed a decline. The present study (F.E.M.) exhibited lower stress amplification factors than the study by Cornwell (2006) for spring curvature indices 2.5, 3.75, 5.0, and 10. For spring index 6.25, the results of both studies converged, while for the spring indices of 7.5 and 8.75, the numerical analysis showed higher values. This difference can be related to the type of mesh used in each study, which directly influences the modeling results and its size, which can be a limiting factor for the analysis. Equation 11 adjusts the data obtained in the present study to the stress amplification factor for the square section wire spring.

$$K = e^{[0{,}9633-0{,}7246.lnC+0{,}2003.(lnC)^2-0{,}0181.(lnC)^3+0{,}0006.(lnC)^4]} \quad (11)$$

4.2 Buckling analysis

Figure 7a shows the stability curve for the spring with a circular section wire, with a free end for rotation in the axis perpendicular to the longitudinal. The study presented intermediate results compared to the results of studies by Haringx (1948) and A.S.D. Handbook (1987). For larger free length/coil diameter ratios, greater susceptibility to unstable behavior was shown, which could eventually result in buckling failure. Furthermore, when this ratio is between 6 and 10, it approaches the values found by A.S.D. Handbook (1987). When this ratio decreases to values between 3 and 5, their behavior approaches stability. However, they do not become close enough. In this way, your best results are situated in the mean value between the other two present results. Furthermore, the deflection ratio value that is greater than 50% is due to the type of analysis that was linear.

With both ends set fixed, where there is the possibility of deflection (Fig. 7b), the spring continues to present intermediate values between the results of studies by Haringx (1948) and A.S.D. Handbook (1987), presenting values more susceptible to buckling failure when the ratio is between 7 and 10, in which these points are close to those provided by A.S.D. Handbook (1987). At points with a ratio of 4 and 5, there is greater stability, where the ratio with a value of 4 converges with the results of Haringx (1948). Furthermore, for the minimum aspect ratio value, a deflection ratio greater than 90% was obtained, a very unusual result compared to another condition, which may have occurred due to the type of analysis.

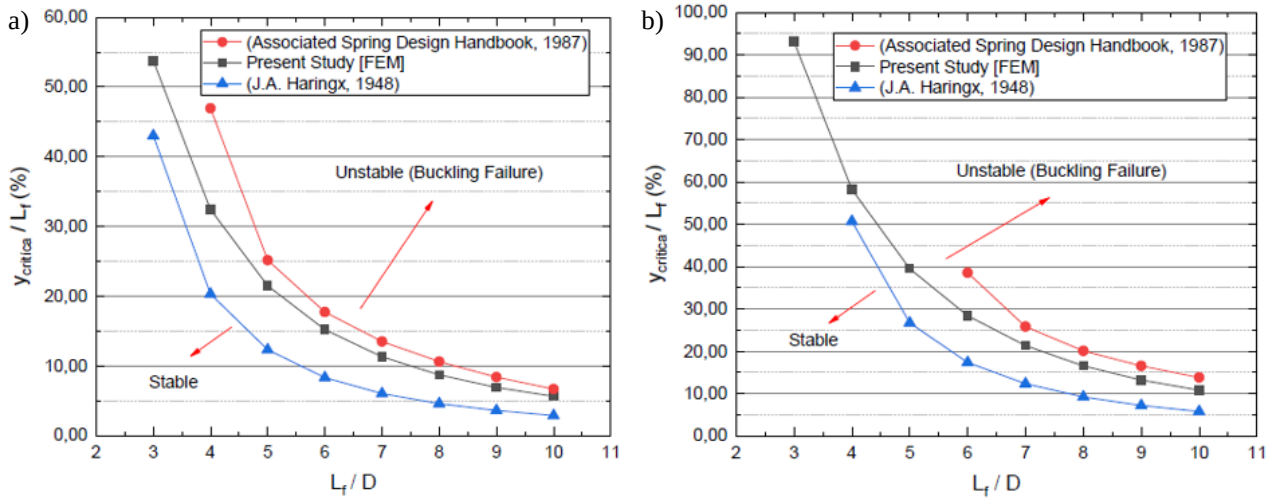

Figure 7. Stability curve for buckling failure for spring with circular section wire. a) One end set fixed and one end with a pin. b) Both ends are fixed (Own Authorship, 2021).

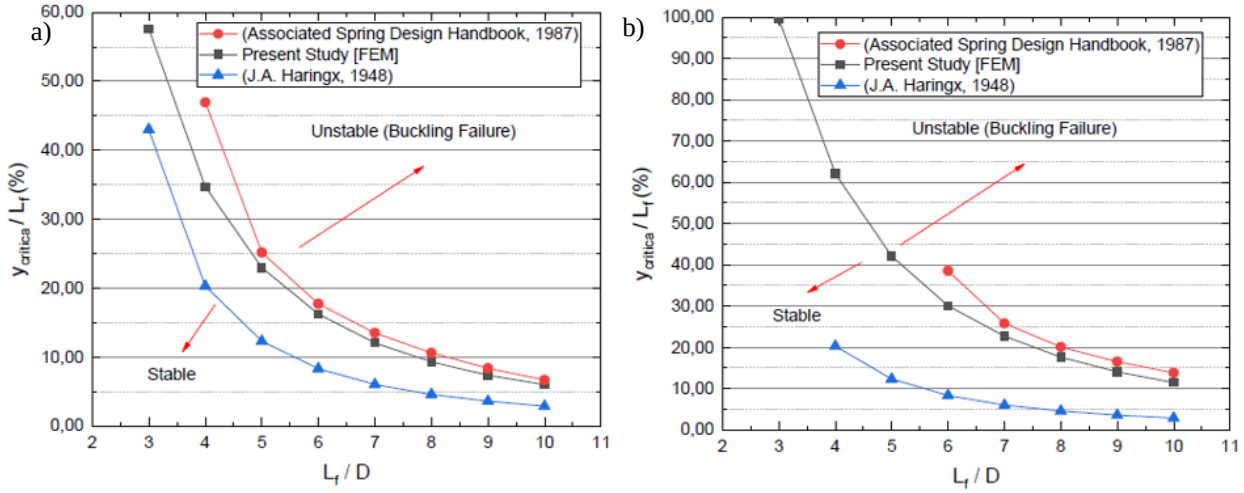

Figure 8. Stability curve for buckling failure for spring with square section wire. a) One end set fixed and one end with a pin. b) Both ends are fixed (Own Authorship, 2021).

Figure 8a shows that the stability curve for the spring with a square-section wire, with a free end for rotation perpendicular to the longitudinal axis, has intermediate results compared to the results of studies by Haringx (1948) and A.S.D. Handbook (1987). For higher free length/coil diameter ratios, the numerical analysis showed greater susceptibility to unstable behavior, resulting in buckling failure. Furthermore, when this ratio is between 5 and 10, it comes even closer to the values provided by A.S.D. Handbook (1987), when compared to the circular section for the same condition. However, when this ratio decreases to values between 3 and 4, its behavior becomes closer to Haringx (1948) results, but they are not close enough. In this way, your best results are situated close to the intermediate value between the other two present results. However, it is observed that its deflection ratio value is close to 60%, which, as in the previous analysis, may have occurred due to the type of analysis used (linear).

With both ends set fixed, with one end allowing deflection (Fig. 8b), the spring continues to present intermediate values between the results of studies by Haringx (1948) and A.S.D. Handbook (1987), presenting values more susceptible to buckling failure when the ratio is between 7 and 10, in which these points are close to the values provided by A.S.D. Handbook (1987), and the results for the circular section for this same condition. However, unlike the study in the circular section, at no point does the present study demonstrate values closer to the results of Haringx (1948), which presents a more stable behavior than those of Handbook (1987) and thus, it can be said that, for this geometry, instability is more likely to occur, thus resulting in buckling failure. Furthermore, it is observed that its deflection ratio reaches 100% due to the type of analysis (linear). However, high ratio values mean that it is necessary to use higher loads for buckling to occur.

5. CONCLUSION

Based on the above, some conclusions are reached regarding buckling. Square section springs showed better results in the numerical analysis, and this could be motivated by their geometry, which has a higher elastic constant. The type of analysis performed directly influenced the results, as there was a limitation to model the change in stiffness of the elements during the buckling study. However, the results obtained corroborate the results already existing in the literature.

As for the stress analysis, it is observed that the direct shear factor and stress concentration were different for the types of sections studied. For the analysis of the circular section, it was seen that the present study presented greater voltage amplification than the studies to which it was being compared. Thus, it can be said that they were more conservative results and will present greater security in applications. Furthermore, even if it presented higher values, there was a convergence between the compared results, thus validating the results obtained. Finally, in the square section analysis, it is observed that there are few studies carried out in this regard, and it is important to emphasize the relevance of studies on this subject. The analysis performed showed lower values than the study with which it was compared, thus implying that the literature used for comparison presents more conservative values, thus validating this literature.

6. ACKNOWLEDGMENT

We gratefully acknowledged the Federal University of Ceará Campus de Russas for supporting and encouraging scientific research and to Professor Ms. Ramon Rudá Brito Medeiros, who has always provided high-quality teaching.

7. REFERENCES

Alves Filho, A., Elementos Finitos: a base da tecnologia CAE. São Paulo: Editora Érica Ltda, 2007.

Ansys R1, Help System, Eigenvalue Buckling Analysis, 2021.

Associated Spring Design Handbook: Engineering Guide to Spring Design. Associated Spring, Barnes Group Inc., Bristol, Conn., 1987.

Cornwell, R. E., Stress Concentration Factors for the Torsion of Curved Beams of Arbitrary Cross Section. Proc. Inst. Mechanical Engineers — Part C — Journal of Mechanical Engineering Science; Dec2006, Vol. 220 Issue 12, pp.1709–1726.

Haringx, J.A., On Highly Compressible Helical Springs and Rubber Rods and Their Application for Vibration-Free Mountings, I e II, *Phillips Res. Rep.*, v. 3, dez. 1948, p. 401 - 449, v. 4, fev. 1949, p. 49 - 80.

Haubert, G. G., Estudo de análises linear e não linear aplicado à flambagem. Universidade Tecnológica Federal do Paraná. 2017.

Henrici, P., On helical springs of finite thickness. Quart. Appl. Math., 1955, 13, 106–110.

Logan, D. L., A First Course in the Finite Element Method. 2ed. PWS Kent: Boston, 1992.

Norton, R.L., Projeto de Máquinas: uma abordagem integrada, 4° edição, 2013.

Rao, S.S., Vibrações Mecânicas, 6° edição, 2016.

Wahl, A.M., Mechanical Springs, 1° edição. Nova York, McGraw-Hill, 1963.

8. DECLARATION OF COMPETING INTEREST

The authors are solely responsible for the printed material included in this paper.